Development of mathematical model to predict the ultimate tensile strength of friction stir welded dissimilar aluminum alloy

R. Palanivel*, P. Koshy Mathews**, N. Murugan***

*Kalaivani College of Technology, Palathurai, Coimbatore, 641105, India, E-mail: rpelmech@yahoo.co.in
**Kalaivani College of Technology, Palathurai, Coimbatore, 641105, India, E-mail: pkoshymathews@yahoo.co.in
***Coimbatore Institute of Technology, Coimbatore, 641014, India, E-mail: drmurugan@gmail.com

1. Introduction

Friction stir welding (FSW) is a solid state welding process developed by The Welding Institute (UK) in 1991, and now being used increasingly for joining aluminium alloys for which fusion welding is often difficult. FSW uses a rotating tool with a probe travelling along the weld path, and plastically deforming the surrounding material to form the weld. Since the material subjected to FSW does not melt and recast, the resultant weld offers advantages over conventional fusion welds such as less distortion, lower residual stresses and fewer weld defects[1-3]. By developing such technology, one of the most important facts is represented by the possibility of joining different aluminium alloys [4].

Development of sound joints between dissimilar materials is a very important consideration for many emerging applications including the ship building, aerospace, transportation, power generation, chemical, nuclear and electronics industries [5]. However, joining of dissimilar materials by conventional fusion welding is difficult because of poor weldability arising from different chemical, mechanical, thermal properties of welded materials and formation of hard and brittle intermetallic compounds (IMC) in large scale at weld interface. The absence of melting in the FSW provides considerable tends to produce reliable dissimilar joints. Amancio-Filho et al [6] determined the tensile strength of the dissimilar friction stir welded AA2024-T351 and AA6056-T4 as 56 % of the AA2024-T351 and 90% of the AA6056-T4. It is reported that the poor tensile strength observed in these joints are due to the thermal softening of the base metals; and the poor ductility observed in these joints is due to the stress concentration caused by the large difference in strength between base metals, leading to confined plasticity and then failure. Cavaliere et al [4] investigated the tensile behavior of dissimilar friction stir welded joints of aluminium alloys 2024-T3 and 7075-T6; and reported that both the ultimate strength and elongation of the dissimilar joints are lower than both the base metals 2024-T3 and 7075-T6.

Bala Srinivasan et al [7] studied the corrosion susceptibility of dissimilar welds. Lomolino et al [8] indicated that higher welding speeds are associated with low heat inputs, and resulted in faster cooling rates of the welded joint. This can significantly reduce the extent of metallurgical transformations taking place during welding (such as solubilisation, re-precipitation and coarsening of precipitates); and hence, the local strength of individual regions across the weld zone in FSW of Al alloys. The microstructural evolution of dissimilar welds as a function of processing parameters has been widely studied in [9] showing the behavior of AA6061-AA2024 materials.

From the above literature review it is observed that very few research works are carried out in dissimilar FSW of aluminium alloys and those researches are not discussing about dissimilar FSW of AA6351 and AA5083 which is widely used in aerospace, shipbuilding, and other fabrication industries[10]. Since fusion welding processes are not suitable for the dissimilar welding of aluminium alloys, FSW process could be the best for the dissimilar welding of these alloys. For designing a set of experiments, developing a mathematical model, analyzing for the optimum combination of input parameters, and expressing the values response surface method is the most successful method [11]. This approach helps in minimizing the experimental cost and time by conducting the experiments with minimum combination of input parameter at the same time increases the chances of success.

Hence, the present research work focuses on the development of mathematical models to predict the ultimate tensile strength of dissimilar FSW joints of aluminium alloys AA6351-T6 and AA5083-H111. The developed model is tested for its adequacy and accuracy using ANOVA and conformity tests, respectively. The effects of various process parameters, viz. tool pin profile, tool rotational speed, welding speed, and tool axial force on ultimate tensile strength of dissimilar FSW joints are predicted using the developed models.

2. Experimental work

2.1. Identifying the important process parameters

Based on preliminary trials, the independent process parameters affecting the tensile properties were identified as: tool pin profile (P), tool rotational speed (N), welding speed (S) and axial force (F).

2.2. Manufacturing of FSW tools

Five different tools made of High Carbon High Chromium steel (HCHCr) having different pin profile of Straight Square (SS), Tapered Square (TS), Straight Hexagon (SH), Straight Octagon (SO) and Tapered Octagon (TO) without draft were used to weld the FSW joints. Each tool having the configuration of shoulder diameter 18 mm, pin diameter 6 mm and pin length 5.6 mm and shoulder – work piece interference surface – 3 concentric circular equally spaced slots of 2 mm depth on all tools.
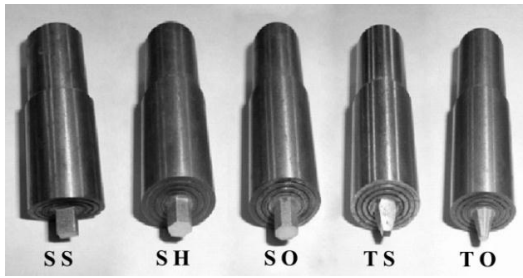
Fig. 1 Manufactured tool for FSW (Straight Square (SS), Straight Hexagon (SH), Straight Octagon (SO), Tapered Square (TS), and Tapered Octagon (TO))
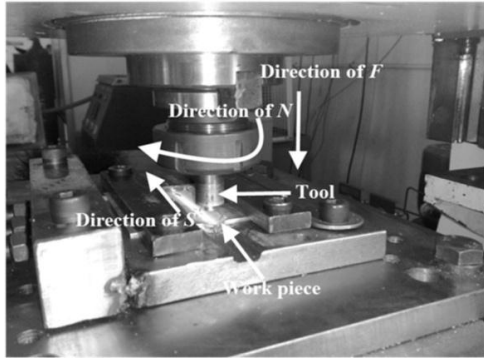

Fig. 2 Experimental setup of FSW

The FSW tools were manufactured using CNC turning centre and wire cut EDM (WEDM) machine to get accurate profile. The tools were oil hardened. The manufactured tools are shown in Fig. 1.

2.3. Finding the limits of control variable

Trial runs were conducted to find the upper and lower limit of process parameters for 6mm thick AA6351-AA5083 aluminum alloy, by varying one of the parameter and keeping the rest of them at constant values. The chemical composition of the materials AA6351-T6 and AA5083-H111 are presented in Tables 1 and 2 respectively. The mechanical properties of the materials are presented in Table 3. Feasible limits of the parameters were chosen in such a way that the joint should be free from visible defects. The upper limit of a factor was coded as +2 and lower limit as -2. The intermediate coded can be calculated from the following relationship.

$$X_i = 2 [2X-(X_{max}+X_{min})] / (X_{max} - X_{min})$$

where X_i is the required coded value of a variable X and X is any value of the variable from X_{min} to X_{max}; X_{min} is the lower limit of the variable and X_{max} is the upper limit of the variable. The selected FSW process parameters with their limits, units and notations are given in Table 4.

2.4. Development of design matrix

The selected design matrix is shown in Table 5. It is a four factor five level central composite rotatable designs consisting of 31 sets of coded conditions composed of a full factorial $2^4 = 16$, plus 7 centre points and 8 star points thus 31 experimental runs allowed the estimation of the linear, quadratic and two way interactive effects of the process parameter on the tensile properties.
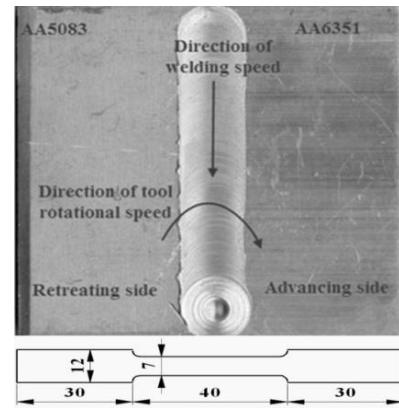

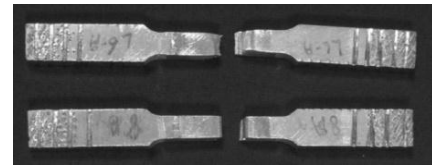Fig. 3 FS welded sample with scheme of preparation of specimen for tensile strength

Fig. 4 Tensile specimen after finding tensile strength

2.5. Conducting the experiment as per the design matrix

The experiments were conducted as per the design matrix with the help of experimental set up as shown in Fig. 2 having dedicated arrangements designed for the FSW. The plate AA 6351-T6 was fixed with the advancing side and AA5083 H-111was fixed with the retreating side of the fixtures of the machine. The tool is plunged into the work piece to be welded while rotating the tool then tool moved over the work piece along the direction of welding speed as shown in Fig. 2.The heating is produced due to friction between the tool and the work piece. The localized heating softens the material around the pin and solid state weld is formed behind the tool. A sample of the FSW plates with scheme of tensile specimen preparation shown in Fig. 3

2.5. Recording of the responses

Tensile test specimens were prepared as per ASTM E8 standard and transverse tensile properties ultimate tensile strength of the FSW joints were evaluated using computerized universal testing machine. For each welded plate, three specimens were prepared and tested. The average values of the results obtained from those specimens are tabulated and presented in Table 5 as experimental value. Fig. 4 shows tensile specimen after finding the tensile strength.

2.6. Development of mathematical model

Ultimate tensile strength (σ_{ut}), of the joints is a function of tool pin profile, tool rotational speed, welding speed, and axial force and it can be expressed as

$$\sigma_{ut} = Y = f(P, N, S, F) \text{ MPa} \qquad (1)$$

where P is function of tool pin profile (Fig. 1); N is rotational speed, rpm; S is welding speed, mm/min; F is axial force, kN.

Chemical composition of AA6351-T6

Name of the element	Si	Zn	Mg	Mn	Fe	Cu	Ti	Al
Weight % (AA6351)	0.907	0.89	0.586	0.65	0.355	0.086	0.015	Balance

Chemical composition of AA5083 –H111

Name of the element	Si	Zn	Mg	Mn	Fe	Cu	Ti	Al
Weight % (AA5083-H111)	0.045	0.04	4.76	0.56	0.14	0.02	0.054	Balance

Mechanical properties of the AA6351 and AA5083-H111

Base material	Tensile strength, MPa	Yield strength, MPa	Percentage of elongation
AA6351	310	285	14
AA5083-H111	308	273	23

FSW Process parameter and its levels

Parameters	Units	Notations	Levels				
Pin profile		P	TS	SH	SS	SO	TO
Rotational speed	rpm	N	600	775	950	1125	1300
Welding speed	mm/min	S	36	49.0	63	76.5	90
Axial force	kN	F	9.81	12.26	14.72	17.17	19.62

The second order polynomial (regression) equation used to represent the response surface "Y" is given by

$$Y = b_0 + \sum b_i x_i + \sum b_{ij} x_i^2 + \sum b_{ij} x_i x_j \qquad (2)$$

The coefficient b_1, b_2 ... b_k are the linear terms, the coefficient b_{11}, b_{22} ... b_{kk} are the quadratic terms and coefficients b_{12}, b_{13} ... b_{k-1}, are the interaction terms. For the four factors, the selected polynomial could be expressed as

$$Y = b_0 + b_1 P + b_2 N + b_3 S + b_4 F + b_{11} P^2 + b_{22} N^2 +$$
$$+ b_{33} S^2 + b_{44} F^2 + b_{12} PN + b_{13} PS + b_{14} PF +$$
$$+ b_{23} NS + b_{24} NF + b_{34} SF \qquad (3)$$

The values of the coefficients are calculated by regression analysis with the help of following equations [11]

$$b_0 = 0.142857 \sum (Y) - 0.035714 \sum \sum (X_{ii} Y) \qquad (4)$$

$$b_j = 0.041667 (X_i Y) \qquad (5)$$

$$b_{ii} = 0.03125 \sum (X_{ii} Y) + 0.00372 \sum \sum (X_{ii} Y) -$$
$$- 0.035714 \sum (Y) \qquad (6)$$

$$b_{ij} = 0.0625 \sum (X_{ij} Y) \qquad (7)$$

DESIGN EXPERT software version 8.0.4 package was used to calculate the values of those coefficients for different responses. After determining the coefficients, the mathematical models were developed.

2.7. Developed final mathematical model

The developed final mathematical model equations in the coded form are given below

$$\sigma_{ut} = 272.78 - 3.15 P + 0.35 N + 2.10 S -$$
$$- 0.03051 F + 6.11 PN - 10.26 P^2 -$$
$$- 11.40 N^2 - 9.22 S^2 + 0.0854 F^2, \text{ MPa.} \qquad (8)$$

2.8. Checking the adequacy of the developed model

The adequacy of the models so developed was then tested by using the analysis of variance technique (ANOVA). The criterion that is commonly used to illustrate the adequacy of a fitted regression model is the coefficient of determination (R^2). For the models developed, the calculated R^2 values and adjusted R^2 values are above 90%. These values indicate that the regression models are quite adequate. The ANOVA test results are given in Table 6. The validity of regression models developed is further tested by drawing scatter diagrams. Typical scatter diagrams for all the models are presented in Fig. 5. The observed values and predicted values of the responses are scattered close to the 45° line, indicating an almost perfect fit of the developed empirical models [12].
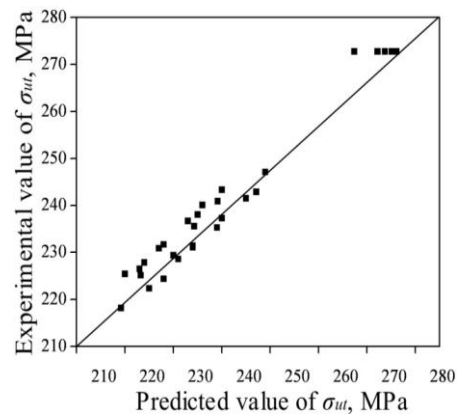

Fig. 5 Scatter diagram for ultimate tensile strength σ_{ut}

Table 5

Design matrix and experimental value with predicted value of ultimate tensile strength

Trail No	FSW Process parameters				σ_{ut}, MPa		
					Experimental value	Predicted value	Error, %
	P	N	S	F			
1	-1	-1	-1	-1	247	242.90	1.73
2	1	-1	-1	-1	228	224.38	1.61
3	-1	1	-1	-1	234	231.38	1.13
4	1	1	-1	-1	240	237.30	1.13
5	-1	-1	1	-1	249	247.10	0.76
6	1	-1	1	-1	231	228.58	1.05
7	-1	1	1	-1	234	235.58	-0.54
8	1	1	1	-1	245	241.50	1.44
9	-1	-1	-1	1	233	236.68	-1.55
10	1	-1	-1	1	219	218.16	0.46
11	-1	1	-1	1	223	225.16	-0.84
12	1	1	-1	1	234	231.08	1.26
13	-1	-1	1	1	239	240.88	-0.72
14	1	-1	1	1	225	222.36	1.18
15	-1	1	1	1	230	229.36	0.27
16	1	1	1	1	239	235.28	1.58
17	-2	0	0	0	235	238.04	-1.27
18	2	0	0	0	220	225.44	-2.41
19	0	-2	0	0	223	226.48	-1.53
20	0	2	0	0	224	227.88	-1.70
21	0	0	-2	0	228	231.70	-1.59
22	0	0	2	0	236	240.10	-1.70
23	0	0	0	-2	240	243.32	-1.36
24	0	0	0	2	227	230.88	-1.68
25	0	0	0	0	272	272.78	-0.21
26	0	0	0	0	276	272.78	1.21
27	0	0	0	0	267	272.78	-1.97
28	0	0	0	0	275	272.78	0.85
29	0	0	0	0	273	272.78	0.33
30	0	0	0	0	272	272.78	-0.23

$$\text{Error, \%} = \frac{\text{Experimental values} - \text{Predicted value}}{\text{Predicted values}} \times 100$$

Table 6

ANOVA test results

Response	Sum of squares		Mean squares		Degrees of freedom		F-Ratio	R^2 value	Adjusted R^2 value
	Regression	Residual	Regression	Residual	Regression	Residual			
UTS	9093.16	260.81	1010.35	13.04	9	20	77.48	0.97	0.95

Table 7

Results of conformity test for ultimate tensile strength

FSW parameters				Experimental values σ_{ut}, MPa	Predicted values σ_{ut}, MPa	Error, %
P	N	S	F			
-2	-2	-2	0	178	175.1	1.65
-2	0	0	2	198	196.14	0.94
2	1	1	1	205	207.46	-1.18
0	1	2	1	220	217.02	1.37
-1	0	0	-1	256	259.86	-1.48

2.9. Confirmation experiments

Experiments were conducted to verify the regression Eq. (8). Five weld runs are made using different values of rotational speed, welding speed and axial force other than what were used in the design matrix. The results obtained are quite satisfactory and the details are presented in Table 7.

3. Analysis of the results

The effects of the different process parameter on the tensile strength of FS welded dissimilar aluminum alloy AA6351-AA5083 are predicted from the mathematical models using the experimental observations are presented in Figs. 6-9 showing the general trends between cause and effect.

3.1. Effect of rotational speed (N)

Fig. 6 shows the direct effect of rotational speed on tensile strength. At lower rotational speed (600 rpm) tensile strength of the FSW joints is lower. When the rotational speed is increased from 600 rpm, correspondingly the tensile strength also increased and reached a maximum at 950 rpm. If the rotational speed is increased above 950 rpm, the tensile strength of the joint is decreased. A decrease in tool rotation speed reduces the area of the weld zone and affects the temperature distribution in the weld zone and produces low heat input. This lower heat input condition resulted in lack of stirring and yielded lower joint strength. It is clear that in FSW as the rotational speed increases the heat input also increases. More heat input destroys the regular flow behaviour and higher rotational speed causes excessive release of stirred materials to the upper surface, which left voids in the weld zone [13].
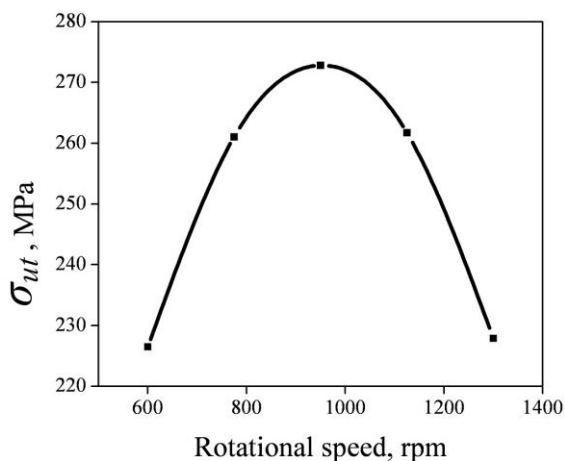

Fig. 6 Dependence of ultimate tensile strength σ_{ut} on tool rotational speed

3.2. Effect of welding speed (S)

Fig. 7 shows the effect of welding speed on tensile strength of FSW dissimilar aluminum alloy. At lower welding speed (36 mm/min), tensile strength of the FSW joints is lower. When the welding speed is increased from 36 mm/min, correspondingly the tensile strength also increased and reached a maximum at 63 mm/min. If the welding speed is increased above 63 mm/min, the tensile strength of the joint is decreased. This is due to the increased frictional heat and insufficient frictional heat generated respectively [14].
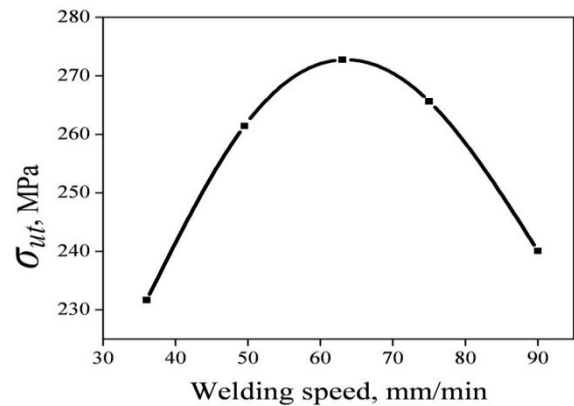

Fig. 7 Dependence of ultimate tensile strength σ_{ut} on welding speed

In general, FSW at higher welding speeds results in short exposure time in the weld area with insufficient heat and poor plastic flow of the metal and causes some voids like defects in the joints. The reduced plasticity and rates of diffusion in the material may have resulted in a weak interface also higher-welding speeds that are associated with low heat inputs, which result in faster cooling rates of the welded joint hence yielded lower tensile strength.

3.3. Effect of axial force (F)

Fig. 8 shows the effect of axial force on tensile strength of friction stir welded dissimilar aluminium alloy. At lower axial force (9.81 kN) tensile strength of the FSW joints is lower. When the axial force is increased from 9.81 kN, correspondingly the tensile strength is also increased and reached a maximum at 14.72 kN. If the axial force is further increased above 14.72 kN, the tensile strength of the joint is decreased. The increase in the tool axial force leads to the increase in the frictional heat generated and increase in the plunge depth of the tool into the work pieces [9, 14]. This may be due to insufficient coalescence of transferred material [15].
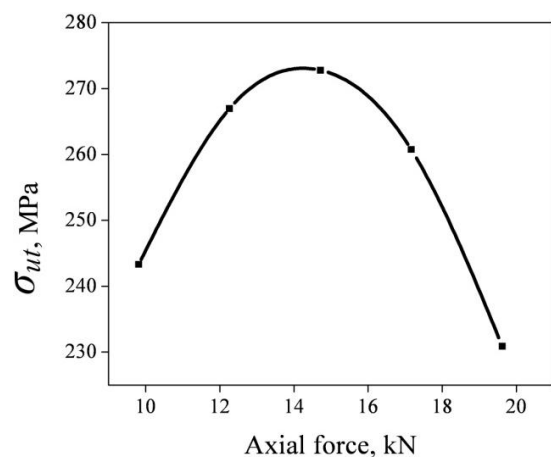

Fig. 8 Dependence of ultimate tensile strength σ_{ut} on axial force

3.4. Effect of pin profile

Fig. 9 shows the effect of tool pin profile on tensile strength of friction stir welded dissimilar aluminium alloy. The joint welded by using straight square tool pin profile has higher tensile strength compared to other tool pin profile. The relationship between the static volume and dynamic volume decides the path for the flow of plasticized material from the leading edge to the trailing edge of the rotating tool [13]. This ratio is equal to1.56 for Straight Square, 1.21 for straight hexagon, 1.11 for straight octagon, 2.04 for tapered octagon 3.51 for tapered square pin profiles. In addition, those pin profiles produce a pulsating stirring action in the flowing material due to flat faces.
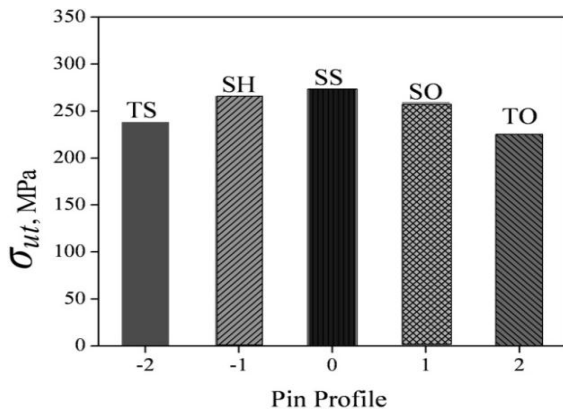

Fig. 9 Dependence of ultimate tensile strength σ_{ut} on pin profile

The square pin profile produces 63 pulses/s, hexagon pin profile produces 95 pulses/s and octagon pin profile produces 126 pulses/s, when the tool rotates at a speed of 950 rpm. There is not much pulsating action in the case of octagonal and hexagonal pin profiled tool because it almost resembles a straight cylindrical pin profiled tool at this high rpm. In the tapered pin profiled tools, the same principle affects the material flow. Since the tapered square and tapered octagon pin profile sweeps less material when compared to that of straight square pin tool, this joint exhibit less tensile properties.

4. Conclusions

The following conclusions are arrived at from the above investigations.

1. Friction stir welding tools with five different pin profiles were developed successfully which are suitable for the dissimilar FS welding of aluminium alloys. The working range of operating parameters for a good quality dissimilar FS welded joints of aluminium alloys AA6351-T6 and AA5083-H111 was found.

2. Regression modelling equations were developed based on the experimental values of ultimate tensile strength of the dissimilar FS welded aluminium alloys AA6351-T6 and AA5083-H111, and they were validated.

3. Based on the regression models the effects of FSW parameters on ultimate tensile strength of the dissimilar FS welded joints were presented and interpreted in detail.

4. The joints fabricated using Straight Square(SS) pin profiled tool with a rotational speed of 950 rpm, welding speed of 63 mm/min and axial force of 14.72 kN exhibited superior tensile properties were compared to other joints.

References

1. **Mishraa, R.S.; Ma, Z.Y.** 2005. Frictions stir welding and processing, Materials Science and Engineering: R: Reports 50(1-2): 1-78.
http://dx.doi.org/10.1016/j.mser.2005.07.001.

2. **Nandan, R.; DebRoy, T.; Bhadeshia, H.K.D.H.** 2008. Recent advances in friction-stir welding process, weldment structure and properties, Progress in Material Science 53: 980-1023.
http://dx.doi.org/10.1016/j.pmatsci.2008.05.001.

3. **Uematsu, Y.; Tokaji, K.; Shibata, H.; Tozaki, Y.; Ohmune, T.** 2009. Fatigue behavior of friction stir welds without neither welding flash nor flaw in several aluminium alloys; International Journal of Fatigue 31: 1443-1453.
http://dx.doi.org/10.1016/j.ijfatigue.2009.06.015.

4. **Cavaliere, P.; Cerri, E.; Squillace, A.** 2005. Mechanical response of 2024-7075 aluminium alloys joined by Friction Stir Welding, Journal of Material Science 40: 3669-76.
http://dx.doi.org/10.1007/s10853-005-0474-5.

5. **Saeid, T.; Abdollah-zadeh, A.; Sazgari, B.** 2010. Weldability and mechanical properties of dissimilar aluminum–copper lap joints made by friction stir welding, Journal of Alloys and Compounds 490: 652-655.
http://dx.doi.org/10.1016/j.jallcom.2009.10.127.

6. **Amancio-Filho, S.T.; Sheikhi, S.; Dos Santos, J.F.; Balfarini, C.** 2008. Preliminary study on the microstructure and mechanical properties of dissimilar friction stir welds in aircraft aluminium alloys 2024-T351 and 6056-T4, Journal of Material processing Technology 206: 32-42.

7. **Bala Srinivasan, P.; Dietzel, W.; Zettler, R.; Dos Santos, J.F.; Sivasan, W.** 2005. Stress corrosion cracking susceptibility of friction stir welded AA7075-AA6056 dissimilar joint, Material Science Engineering A 392: 292300.
http://dx.doi.org/10.1016/j.msea.2004.09.065.

8. **Lomolino, S.; Tovo, R.; Dos Santos, J.** 2005. On the fatigue behavior and design curves of friction stir butt welded Al alloys, International Journal of Fatigue 27: 305-316.
http://dx.doi.org/10.1016/j.ijfatigue.2004.06.013.

9. **Ouyang, J.H.; Kovacevic, R.** 2002. Material flow and microstructure of the friction stir butt welds of the same and dissimilar aluminum alloys, Journal of Material Engineering Performance 11: 51-63.
http://dx.doi.org/10.1007/s11665-002-0008-0.

10. **Chandler, H.D.; Bee, J.V.** 1987. Cyclic strain induced precipitation in a solution treated aluminum alloy, Acta Metallurgica 35: 2503-2510.
http://dx.doi.org/10.1016/0001-6160(87)90147-7.

11. **Gunaraj, V., Murugan, N.** 1999. Application of response surface methodology for predicting weld bead quality in submerged arc welding of pipes, Journal of Material Processing Technology 88: 266-275.
http://dx.doi.org/10.1016/S0924-0136(98)00405-1.

12. **Kim, I.S.; Son, K.J.; Yang, Y.S.; Yaragada, P.K.D.V.** 2003. Sensitivity analysis for process parameter para-

meters in GMA welding process using factorial design method, International Journal of Machine Tools and Manufacture 43: 763-776.
http://dx.doi.org/10.1016/S0890-6955(03)00054-3.

13. **Elangovan, K.; Balasubramanian, V.** 2007. Influences of pin profile and rotational speed of the tool on the formation of friction stir processing zone in AA2219 aluminum alloy, Material Science Engineering A 459: 7-18.
http://dx.doi.org/10.1016/j.msea.2006.12.124.

14. **Colligan, J.; Konkol, Paul J.; Fisher, James J.; Pickens, Joseph R.** 2002. Friction stir welding demonstrated for combat vehicle construction, Welding Journal, 1-6.

15. **Elangovan, K.; Balasubramanian, V. Valliappan, M.** 2008. Influences of tool pin profile and axial force on the formation of friction stir processing zone in AA6061 aluminium alloy, International Journal of Advanced Manufacturing Technology 38: 285-295.
http://dx.doi.org/10.1007/s00170-007-1100-2.

P. Palanivel, P. Koshy Mathews, N. Murugan

TRINTINIU SUVIRINIMU SUJUNGTŲ SKIRTINGŲ ALIUMINIO LYDINIŲ TEMPIMO STIPRIO RIBOS NUSTATYMO MATEMATINIO MODELIO SUKŪRIMAS

R e z i u m ė

Trintiniu suvirinimu aliuminio jungtis galima sudaryti greičiau ir patikimesnes. Šiame straipsnyje aprašomas sisteminis požiūris, kuriuo remiamasi kuriant skirtingų aliuminio lydinių (AA6351 T6-AA 5083H111) jungčių tempimo stiprio ribos nustatymo matematinį modelį. Naudojami tokie trintinio suvirinimo parametrai kaip įrankio antgalio profilis, įrankio sukimosi greitis, suvirinimo greitis ir ašinė jėga. Eksperimentas buvo atliktas naudojant keturis kintamuosius ir penkis lygius centrinėje besisukančioje projektavimo matricoje. Modeliui kurti buvo taikomas paviršiaus reakcijos metodas. Sukurto modelio tikslumui nustatyti buvo atlikta kintamųjų dispersijos analizė ir patikrinamieji bandymai. Detaliai aptarta trintinio suvirinimo proceso parametrų įtaka trintimi suvirintų skirtingų jungčių tempimo stiprio ribai.

R. Palanivel, P. Koshy Mathews, N. Murugan

DEVELOPMENT OF MATHEMATICAL MODEL TO PREDICT THE ULTIMATE TENSILE STRENGTH OF FRICTION STIR WELDED DISSIMILAR ALUMINUM ALLOY

S u m m a r y

Development of the Friction Stir Welding (FSW) has provided an alternative improved way of producing aluminium joints, in a faster and reliable manner. This paper presents a systematic approach to develop a mathematical model for predicting the Ultimate Tensile Strength (UTS) of dissimilar aluminum alloy (AA6351 T6 - AA5083 H111) joints by incorporating the Friction Stir Welding (FSW) process parameter such as tool pin profile, tool rotational speed, welding speed, and axial force. The experiment was conducted based on four factors five level central composite rotatable deign with full replication technique. The Response Surface Method (RSM) was employed to develop the model. The developed model was validated using the statistical tool analysis of variance (ANOVA). Conformity tests were carried out to check the accuracy of the developed model. The effects of the FSW process parameters on ultimate tensile strength of friction welded dissimilar joints were discussed in detail.